

This is the accepted manuscript made available via CHORUS. The article has been published as:

# Polarization observables in the longitudinal basis for pseudo-scalar meson photoproduction using a density matrix approach

Biplab Dey, Michael E. McCracken, David G. Ireland, and Curtis A. Meyer

Phys. Rev. C **83**, 055208 — Published 26 May 2011

DOI: [10.1103/PhysRevC.83.055208](https://doi.org/10.1103/PhysRevC.83.055208)

# Polarization observables in the longitudinal basis for pseudo-scalar meson photoproduction using a density matrix approach

Biplab Dey,<sup>1</sup> Michael E. McCracken,<sup>1,2</sup> David G. Ireland,<sup>3</sup> and Curtis A. Meyer<sup>1</sup>

<sup>1</sup>*Carnegie Mellon University, Pittsburgh, Pennsylvania 15213, USA*

<sup>2</sup>*Washington & Jefferson College, Washington, Pennsylvania 15301, USA*

<sup>3</sup>*University of Glasgow, Glasgow G12 8QQ, United Kingdom*

The complete expression for the intensity in pseudo-scalar meson photoproduction with a polarized beam, target, and recoil baryon is derived using a density matrix approach that offers great economy of notation. A Cartesian basis with spins for all particles quantized along a single direction, the longitudinal beam direction, is used for consistency and clarity in interpretation. A single spin-quantization axis for all particles enables the amplitudes to be written in a manifestly covariant fashion with simple relations to those of the well-known CGLN formalism. Possible sign discrepancies between theoretical amplitude-level expressions and experimentally measurable intensity profiles are dealt with carefully. Our motivation is to provide a coherent framework for coupled-channel partial-wave analysis of several meson photoproduction reactions, incorporating recently published and forthcoming polarization data from Jefferson Lab.

PACS numbers: 24.70.+s, 42.25.Ja, 21.10.Hw, 25.20.-x, 14.40.Aq

## I. INTRODUCTION

The production amplitude for pseudo-scalar meson photoproduction involves eight complex amplitudes which depend on the spin states of the photon and the target and final-state baryons. The reaction can be simplified by considering the parity invariance of the strong and electromagnetic interactions, reducing the number of independent complex amplitudes to four. Barker, Donachie, and Storrow (BDS) [1] showed that there exist fifteen experimentally observable single- and double-polarization observables which, in addition to the differential cross-section, can be expressed as bilinears in the four independent amplitudes. Several ambiguities originate with the BDS work. The BDS article treats reactions with the four amplitudes in the helicity basis (non-flip,  $N$ , double-flip,  $D$ , and two single-flip amplitudes,  $S_1$  and  $S_2$ ), but does not clearly specify to which helicity configurations the amplitudes  $S_1$  and  $S_2$  refer. Other authors [2, 3] follow different schemes for enumerating the four amplitudes.

Chiang and Tabakin (CT) [4] later showed that to completely characterize the full production amplitude, measurements of the differential cross-section and a carefully chosen set of only seven polarization observables is required; that is, there is redundancy in the full set of sixteen bilinear observables. The CT study assumes “measurements” are made with infinite precision, a situation obviously unattainable by any experiment. More recently, the effects of uncertainty in polarization measurements on constraining amplitudes have been studied from an information-theory perspective [5].

Sandorfi *et al.* [6] have pursued descriptions of the polarization observables in terms of the Chew-Goldberger-Low-Nambu (CGLN) amplitudes [7]. They have tested configurations of production amplitudes which reproduce available polarization data for the reaction  $\gamma p \rightarrow K^+ \Lambda$  to

within experimental uncertainties by randomly sampling the amplitude space and projecting observables from the amplitudes. Their work shows that the currently observed set of polarization observables and experimental uncertainties do not provide enough constraint to distinguish between production models containing different resonance contributions, thus suggesting that measurement of a larger number of observables than prescribed by CT will be required to fully extract the four complex amplitudes.

The scope of the present work is three-fold. First, we derive the general expression for the reaction intensity with all three polarizations (beam, target, and recoil). Our motivation is the density matrix approach of Fasano, Tabakin, and Saghai (FTS) [3], the power of which is compactness of notation. The full expression consists of  $4 \times 4 \times 4 = 64$  terms. Invariance under mirror symmetry transformations (a parity inversion followed by a rotation, see Sec. V) removes half of these terms. In the remaining terms, each of the sixteen physically measurable observables occurs twice. All results herein follow simply from the properties of the Pauli matrices and the mirror symmetry operator acting on the spin density matrices of the photon and the baryons.

Second, we provide amplitude-level expressions for the polarization observables corresponding to measurable particle momentum distributions, carefully keeping track of the relative signs between experimental measurements and amplitude-level expressions. Our amplitudes are constructed in the longitudinal basis, that is, with spin projections for all particles quantized along a single direction, the beam direction. For reactions with multiple decays and non-zero spins for the final-state particles, a single spin-quantization axis enables one to write the full production amplitude in a manifestly Lorentz-invariant fashion. A relevant example of such a process is the reaction chain  $\gamma p \rightarrow K^+ \Sigma^0 \rightarrow K^+ \Lambda \gamma_f \rightarrow K^+ p \pi^- \gamma_f$ .

Finally, we list and numerically validate the various

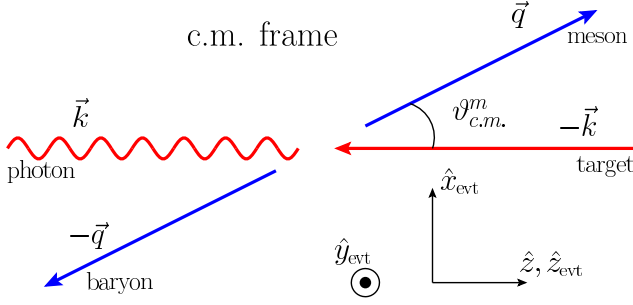


FIG. 1: (Color online) Axes for pseudo-scalar meson photoproduction in the center-of-mass (c.m.) frame for a particular event. The  $z$ -axis is along the photon momentum direction and the  $y$ -axis is normal to the reaction plane. Momenta of the incoming (outgoing) particles are shown in bold red (blue) arrows.  $\vartheta_{c.m.}^m$  is the polar meson-production angle in the c.m. frame. See text for details.

“consistency relations” connecting the different spin observables. These consistency relations provide important checks for both theoretical analyses and constraints in the case of future experiments which will have access to polarizations of the beam and target and recoil baryons.

We aim to establish a consistent partial-wave-analysis formalism for recent [9–13] and future [14, 15] meson photoproduction data from CLAS, as well as all presently available polarization data from other experiments such as GRAAL [16, 17] and LEPS [18–20]. To ensure correct interpretation of these observables, one must be confident of the relationship between measurements extracted from momentum distribution asymmetries and the polarization observables as treated in theoretical studies. Until now, most of the world data on polarizations has been limited by statistics and kinematic coverage. Furthermore, experimental limitations have restricted measurement to only a few of the fifteen polarization observables. However, with a new generation of experiments at Jefferson Lab on the horizon [14, 15], much activity is anticipated in the field in the coming years. This article will provide a self-contained and comprehensive description of the formalism for pseudo-scalar meson photoproduction from the fundamental derivations and a careful treatment of the connection between theory and measurement of polarization observables.

## II. AXIS CONVENTIONS

In the case of single pseudo-scalar meson photoproduction, let  $\vec{k}$ ,  $-\vec{k}$ ,  $\vec{q}$  and  $-\vec{q}$  be the momenta of the incoming photon, target baryon, outgoing meson, and outgoing baryon, respectively, in the overall center-of-mass (c.m.) frame (see Fig. 1). The beam direction defines the  $z$ -axis,  $\hat{z}_{\text{evt}} = \vec{k}/|\vec{k}|$ . The  $y$ -axis is taken to be normal to the reaction plane established by the photon and meson momenta,  $\hat{y}_{\text{evt}} = \vec{k} \times \vec{q}/|\vec{k} \times \vec{q}|$ . The  $x$ -axis is then simply

$\hat{x}_{\text{evt}} = \hat{y}_{\text{evt}} \times \hat{z}_{\text{evt}}$ . Here the subscript “evt” denotes that these axes, with  $\hat{x}_{\text{evt}}$  and  $\hat{y}_{\text{evt}}$  parallel and perpendicular to the reaction plane, are defined on an event-by-event basis.

## III. THE PHOTON POLARIZATION STATE AND DENSITY MATRIX

There is some disparity between the optics and particle-physics communities in the nomenclature of the right- and left-handed polarization states. Particle physicists define the right-handed polarization state following the right-hand rule for the transverse electric polarization vector. The spin of the photon points along its momentum for the right-handed polarization state (or positive helicity state). The left-handed polarization state has the photon spin anti-parallel to its direction of motion. The optics community swaps the definitions for the right- and left-handed states, though the notions of positive- and negative-helicity states are the same in both treatments. Here, we adhere to the particle-physics convention.

We will define the polarization basis states for the photon as

$$|\epsilon_{\text{evt}}^+\rangle = -(|\hat{x}_{\text{evt}}\rangle + i|\hat{y}_{\text{evt}}\rangle)/\sqrt{2} \quad (1a)$$

$$|\epsilon_{\text{evt}}^-\rangle = (|\hat{x}_{\text{evt}}\rangle - i|\hat{y}_{\text{evt}}\rangle)/\sqrt{2}, \quad (1b)$$

where  $|\epsilon^+\rangle$  is the right-handed (positive-helicity) state,  $|\epsilon^-\rangle$  is the left-handed (negative-helicity) state, and  $|\hat{x}_{\text{evt}}\rangle$  and  $|\hat{y}_{\text{evt}}\rangle$  are states of transverse polarization along  $\hat{x}_{\text{evt}}$  and  $\hat{y}_{\text{evt}}$ , respectively. Looking *into* the incoming beam, the  $y$ -component phase leads (trails) the  $x$ -component phase for the positive (negative) helicity states and the polarization vector rotates counter-clockwise (clockwise) for the positive (negative) helicity states, in accordance with the right-hand rule.

For a general mixed state, it is useful to switch to the density-matrix notation for describing the polarization state of the photon. We follow the work of Adelseck and Saghai (AS) [21] and FTS [3] and write the photon spin density matrix as

$$\begin{aligned} \rho^\gamma &= \frac{1}{2} \begin{bmatrix} 1 + P_C^\gamma & -P_L^\gamma \exp(-2i(\theta - \varphi)) \\ -P_L^\gamma \exp(2i(\theta - \varphi)) & 1 - P_C^\gamma \end{bmatrix}_{\text{AS}} \\ &= \frac{1}{2} \begin{bmatrix} 1 + P_z^S & P_x^S - iP_y^S \\ P_x^S + iP_y^S & 1 - P_z^S \end{bmatrix}_{\text{FTS}}. \end{aligned} \quad (2)$$

In the AS prescription, the quantities  $P_L^\gamma$  and  $P_C^\gamma$  denote the degree of linear ( $L$ ) and circular ( $C$ ) polarization. In the FTS treatment,  $\vec{P}^S$  is the so-called Stokes’ vector, common in optics. The kinematic variable  $\varphi$  is the azimuthal angle between the reaction plane and the laboratory  $\hat{x}_{\text{lab}}$  for a linearly polarized photon for a given event. The linear polarization vector relative to the laboratory frame is

$$\hat{n}_{\text{pol}} = \cos \theta \hat{x}_{\text{lab}} + \sin \theta \hat{y}_{\text{lab}}. \quad (3)$$

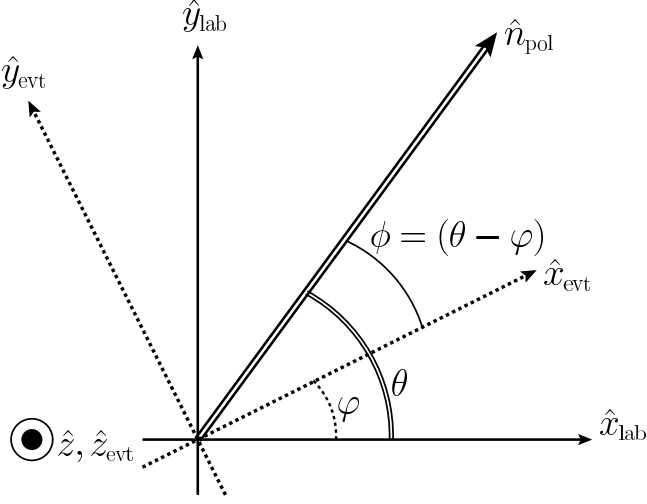


FIG. 2: For a linearly polarized beam,  $\{\hat{x}_{\text{lab}}, \hat{y}_{\text{lab}}, \hat{z}_{\text{lab}}\}$  defines the fixed laboratory axis of the experiment. The polarization direction ( $\hat{n}_{\text{pol}}$ ) is at an angle  $\theta$  to the laboratory  $x$ -axis. For a given event, the reaction plane is at angle  $\varphi$  to the laboratory  $x$ -axis. Therefore, the polarization vector is at an angle  $\phi = (\theta - \varphi)$  relative to the reaction plane.

For the circularly polarized photon (or unpolarized beam) case, the production amplitude is azimuthally symmetric about the beam direction. However, for the linearly polarized case,  $\hat{x}_{\text{lab}}$  and  $\hat{y}_{\text{lab}}$  define a preferred transverse coordinate system. The experimental conditions define  $\hat{n}_{\text{lab}}$ , and  $\theta = 0^\circ$  ( $90^\circ$ ) corresponds to parallel (perpendicular) plane polarizations according to the experimentalist. For a given event, relative to the reaction plane, the polarization vector is

$$\hat{n}_{\text{pol}} = \cos(\theta - \varphi)\hat{x}_{\text{evt}} + \sin(\theta - \varphi)\hat{y}_{\text{evt}}, \quad (4)$$

and the Stokes' vector  $\vec{P}^S$  may be related to the circular polarization quantities by

$$P_z^S = P_C^\gamma \quad (5a)$$

$$P_x^S = -P_L^\gamma \cos(2\phi) \quad (5b)$$

$$P_y^S = -P_L^\gamma \sin(2\phi) \quad (5c)$$

in the basis formed by  $\{\hat{x}_{\text{evt}}, \hat{y}_{\text{evt}}, \hat{z}_{\text{evt}}\}$  and  $\phi = (\theta - \varphi)$ . The angles  $\varphi$ ,  $\theta$ , and  $\phi$  are shown schematically in Fig. 2 and the connection between  $\vec{P}^S$  and the different polarization states are given in Table I. Apart from the right- ( $r$ ) and left-handed ( $l$ ) circular polarizations, which are our basis states, there are the perpendicular ( $\perp$ ) and parallel ( $\parallel$ ) states, corresponding to photons linearly polarized along the  $y$ - and  $x$ -axes, respectively, and two linearly polarized states at  $\pm 45^\circ$  to the  $x$ -axis (in the  $\hat{x}$ - $\hat{y}$  plane), labeled as  $\pm t$ .

Polarization	$P_x^S$	$P_y^S$	$P_z^S$
( $r$ ) Circular helicity +1	0	0	+1
( $l$ ) Circular helicity -1	0	0	-1
( $\perp$ ) Linear ( $\phi = \pi/2$ )	+1	0	0
( $\parallel$ ) Linear ( $\phi = 0$ )	-1	0	0
( $-t$ ) Linear ( $\phi = -\pi/4$ )	0	+1	0
( $+t$ ) Linear ( $\phi = \pi/4$ )	0	-1	0

TABLE I: Stokes' vector  $\vec{P}^S$  for different photon polarization configurations (adapted from Ref. [3]). The right- ( $r$ ) and left-handed ( $l$ ) circular polarizations are our basis states. The different configurations for the linearly polarized states can be expressed in terms of these basis states.  $\phi$  is the angle the linear polarization direction makes with  $\hat{x}_{\text{evt}}$ . See text for details.

#### IV. THE INTENSITY PROFILE AND $T_{lmn}$ ELEMENTS

We first note that as far as the *theoretical* definitions of the polarization observables are concerned, the only relevant kinematic variables for a given total energy ( $W$ ) in the c.m. frame are the angle between the photon polarization vector and the reaction plane,  $\phi = (\theta - \varphi)$  (for a linearly polarized beam), and the polar meson production angle  $\vartheta_{\text{c.m.}}^m$ . This is because the observables are defined as asymmetries relative to the reaction-plane coordinate system  $\{\hat{x}_{\text{evt}}, \hat{y}_{\text{evt}}, \hat{z}_{\text{evt}}\}$ . It is only when we will need to connect the observables to experimentally measurable intensity distributions, that the orientation between reaction plane, photon polarization vector, and the lab frame (quantified by angles  $\theta$  and  $\varphi$ ) will be required. We will return to this point later in Sec. VIII. In what follows (as in the FTS conventions) we will refer to the Pauli matrices operating in the spin spaces of the beam, target baryon, and outgoing baryon as  $\sigma^\gamma$ ,  $\sigma^i$ , and  $\sigma^b$ , respectively. The density matrices are then given by

$$\rho^\gamma = \frac{1}{2}(1 + \vec{P}^S \cdot \vec{\sigma}^\gamma) \quad (6a)$$

$$\rho^i = \frac{1}{2}(1 + \vec{P}^i \cdot \vec{\sigma}^i) \quad (6b)$$

$$\rho^b = \frac{1}{2}(1 + \vec{P}^b \cdot \vec{\sigma}^b). \quad (6c)$$

The vectors  $\vec{P}^S$ ,  $\vec{P}^i$ , and  $\vec{P}^b$  denote the polarization vectors of the beam, target and recoiling baryon, respectively. If any of the beam, target or recoil polarization is not measured, the corresponding  $\vec{P}$  is the zero vector.

We define  $\mathcal{A}_{m_\gamma m_i m_b}$  to be the reaction amplitude for a particular spin configuration of the photon ( $m_\gamma$ ), target ( $m_i$ ) and baryon ( $m_b$ ), with the spin-quantization axes for all particles along  $\hat{z}$ , the beam direction. For a given photon spin,  $m_\gamma$ , the four  $\mathcal{A}$  amplitudes correspond to the elements of a  $2 \times 2$  matrix  $J_{m_\gamma}$  in the space of transition elements for a target spin state  $|m_i\rangle$  going to the baryon spin state  $|m_b\rangle$ . Therefore the matrix elements of  $J_{m_\gamma}$  are

$(J_{m_\gamma})_{m_b m_i} = \langle m_b | J_{m_\gamma} | m_i \rangle$  and  $J$  and  $\mathcal{A}$  are connected via

$$\langle m_b | J_{m_\gamma} | m_i \rangle = \mathcal{A}_{m_\gamma m_i m_b}. \quad (7)$$

For experiments with “mixed” states  $\rho_{\text{in}}$  and  $\rho_{\text{out}}$  as the initial prepared (input) and final measured (output) configurations connected by the transition operator  $J$ , the intensity profile is proportional to the trace  $\text{Tr}[\rho_{\text{out}} J \rho_{\text{in}} J^\dagger]$ . In the present case,  $\rho_{\text{in}} = \rho^i \otimes \rho^\gamma$  and  $\rho_{\text{out}} = \rho^b$ . Therefore, the most general intensity expression for the profile dependent upon beam, target, and recoil polarizations is given by

$$\mathcal{I} = \mathcal{I}_0 \left( \frac{\text{Tr}[\rho^b J \rho^i \rho^\gamma J^\dagger]}{\text{Tr}[J J^\dagger]/8} \right), \quad (8)$$

where  $\mathcal{I}_0$  is the unpolarized cross-section and the traces are over the beam, target and recoil spins. This derivation can be found in FTS [3] and in an equivalent form, in the paper by Goldstein, *et al.* [22]. The main utility of this formulation is its symbolic compactness which enables easy derivation of other observables and their correlations. In Sec. IX we will describe in detail how to expand these traces to give amplitude-level expressions for the polarization observables.

We now establish a notation for the Pauli matrices and the polarization vectors as four-component vectors, wherein

$$\{\sigma_0, \sigma_1, \sigma_2, \sigma_3\} \equiv \{I, \sigma_x, \sigma_y, \sigma_z\} \quad (9a)$$

$$\{P_0, P_1, P_2, P_3\} \equiv \{1, P_x, P_y, P_z\}. \quad (9b)$$

Since each density matrix in Eqs. 6 has four terms, the full profile in Eq. 8 has  $4 \times 4 \times 4 = 64$  terms. We will also adopt the convention:

$$T_{lmn} \equiv \frac{\text{Tr}[\sigma_n^b J \sigma_m^i \sigma_l^\gamma J^\dagger]}{\text{Tr}[J J^\dagger]}, \quad (10)$$

so that Eq. 8 can be compactly represented as

$$\mathcal{I} = \mathcal{I}_0 \left( \sum_{lmn \in \{0,1,2,3\}} P_l^S P_m^i P_n^b T_{lmn} \right). \quad (11)$$

## V. MIRROR SYMMETRY TRANSFORMATIONS

Following the work of Artru *et al.* [23], we first define the mirror inversion operator

$$M = \Pi \exp(-i\pi J_y), \quad (12)$$

which describes a parity inversion ( $\Pi$ ) followed by a  $180^\circ$  rotation about the  $\hat{y}$  axis. We list the effects of  $M$  on the relevant particle types labeled by their spin and parity quantum numbers,  $J^P$ :

- $J^P = 0^-$  pseudo-scalar meson: Only the parity inversion contributes. Thus,  $M = \Pi = -1$  is a simple sign flip.
- $J^P = \frac{1}{2}^+$  baryons: Here  $\Pi = 1$  and  $J_y = \sigma_2/2$ . Therefore  $M = \Pi \exp(-i\pi J_y) = -i\sigma_2$ . In terms of the spin states, the transformation is given by  $|+\rangle \rightarrow |-\rangle$  and  $|-\rangle \rightarrow -|+\rangle$ .
- $J^P = 1^-$  photon: A  $180^\circ$  rotation about the  $\hat{y}$  axis leaves  $|\hat{y}\rangle$  unchanged but changes  $|\hat{x}\rangle$  to  $|- \hat{x}\rangle$ . Substituting this in Eq. 1a leads to an interchange between  $|\epsilon_{\text{evt}}^+\rangle$  and  $|\epsilon_{\text{evt}}^-\rangle$ . Including  $\Pi = -1$  for a vector particle leads to  $M = -\sigma_1$  for the photon in the Pauli basis. In terms of the spin states, the transformation is  $|\epsilon_{\text{evt}}^+\rangle \leftrightarrow -|\epsilon_{\text{evt}}^-\rangle$ .

There are two main effects of the  $M$  transformation of which we make use. First,  $M$  acting on any  $T_{lmn}$  element results in a reshuffle in the Pauli operators for the incoming states:

$$\{0, 1, 2, 3\} \Rightarrow \{-1, -0, -i3, i2\} \text{ (photon)} \quad (13)$$

$$\{0, 1, 2, 3\} \Rightarrow \{-i2, -3, -i0, 1\} \text{ (target)}. \quad (14)$$

where we have transformed the matrices as

$$\sigma_l \Rightarrow M \sigma_l, \quad l \in \{0, 1, 2, 3\}, \quad (15)$$

$M$  being the corresponding mirror transformation matrix for the particular state. However, Eq. 14 does not quite work for the outgoing baryon density matrix, since the effect of the pseudo-scalar meson in the outgoing system needs to be incorporated as well. For the outgoing meson-baryon system, the reshuffle is given by

$$\{0, 1, 2, 3\} \Rightarrow \{-i2, 3, -i0, -1\} \text{ (outgoing system)}, \quad (16)$$

where we have added an extra sign flip for  $\sigma_1$  and  $\sigma_3$  compared to Eq. 14, that comes from the parity of the pseudo-scalar meson. The  $\sigma_0$  terms do not acquire this extra sign flip, since they physically correspond to the situation where the experiment is “blind” to the spins of the outgoing states. Also, since  $\sigma_2$  is connected to the identity matrix by the  $M$  transform, it does not acquire a sign flip.

Second, the action of  $M$  on the production amplitudes and invariance under this transformation lead to relations between the amplitudes for positive and negative photon helicities:

$$L_1 \equiv \mathcal{A}_{+++} = +\mathcal{A}_{---} \quad (17a)$$

$$L_2 \equiv \mathcal{A}_{++-} = -\mathcal{A}_{--+} \quad (17b)$$

$$L_3 \equiv \mathcal{A}_{+--} = +\mathcal{A}_{-++} \quad (17c)$$

$$L_4 \equiv \mathcal{A}_{+-+} = -\mathcal{A}_{-+-}, \quad (17d)$$

where the four independent amplitudes  $L_i$  will be called the *longitudinal basis amplitudes*.

## VI. CONNECTION WITH THE CGLN AMPLITUDES

The  $L_i$  amplitudes are very closely related to the standard CGLN amplitudes [7], since they are both in the Cartesian basis. We first write the general differential cross-section for polarized beam, target and recoil baryon as

$$\frac{d\mathcal{I}}{d\Omega}(m_\gamma, m_i, m_b) = \frac{1}{(4\pi)^2} \frac{1}{4W^2} \left( \frac{|\vec{q}|}{|\vec{k}|} \right)_{\text{c.m.}} |\mathcal{A}_{m_\gamma m_i m_b}|^2, \quad (18)$$

where we have adopted the Peskin-Schroeder [8] normalization for the Dirac spinors,  $\bar{u}u = 2m$ ,  $m$  being the mass of the particle, and  $W$  is the c.m. energy of the system. In the CGLN approach, the cross-section is written as

$$\frac{d\mathcal{I}}{d\Omega}(m_\gamma, m_i, m_b) = \left( \frac{|\vec{q}|}{|\vec{k}|} \right)_{\text{c.m.}} |\langle m_b | \mathcal{F}_{m_\gamma} | m_i \rangle|^2, \quad (19)$$

which leads to the simple relation:

$$\mathcal{A}_{\lambda m_i m_b} = (8\pi W) \left( \chi^\dagger(m_b) \mathcal{F}(\lambda) \chi(m_i) \right)_{m_b m_i}, \quad (20)$$

where  $\chi(m_i)$  and  $\chi(m_b)$  are the two-component spinors of the initial target and the final baryon, respectively, and  $\lambda = \pm 1$  is the photon helicity. Since the amplitude  $\mathcal{A}$  is a Lorentz invariant quantity, one can calculate this in any reference frame. In the c.m. frame, the matrix  $\mathcal{F}(\lambda)$  is expanded in terms of the four CGLN amplitudes  $F_i$ , as,

$$\begin{aligned} \mathcal{F}(\lambda) = & i(\vec{\sigma} \cdot \hat{\epsilon}_\lambda) F_1 + (\hat{\sigma} \cdot \hat{q})(\hat{\sigma} \times \hat{k}) \cdot \hat{\epsilon}_\lambda F_2 \\ & + i(\hat{\epsilon}_\lambda \cdot \hat{q})(\vec{\sigma} \cdot \hat{k}) F_3 + i(\hat{\epsilon}_\lambda \cdot \hat{q})(\vec{\sigma} \cdot \hat{q}) F_4, \end{aligned} \quad (21)$$

where the unit vectors  $\hat{\epsilon}_\lambda$ ,  $\hat{q}$  and  $\hat{k}$  are in the c.m. frame. Since the  $\lambda = \pm 1$  amplitudes are related via Eq. 17, we only need to calculate the  $F_i$ 's for any of  $\lambda = \pm 1$ . Doing this for  $\lambda = +1$  leads to

$$\mathcal{F}(+1) = \frac{-i}{\sqrt{2}} \begin{bmatrix} sF_3 + csF_4 & 2F_1 - 2cF_2 + s^2F_4 \\ s^2F_4 & -2sF_2 - sF_3 - csF_4 \end{bmatrix}, \quad (22)$$

where we have abbreviated  $s = \sin(\vartheta_{\text{c.m.}}^m)$  and  $c = \cos(\vartheta_{\text{c.m.}}^m)$  in terms of the polar meson production angle in the c.m. frame,  $\vartheta_{\text{c.m.}}^m$  (see Fig. 1). Suppressing any irrelevant overall phase, the connections between the  $L_i$  amplitudes and the CGLN amplitudes  $F_i$  are:

$$L_1 = 4\sqrt{2}\pi W (sF_3 + csF_4) \quad (23a)$$

$$L_2 = 4\sqrt{2}\pi W (s^2F_4) \quad (23b)$$

$$L_3 = 4\sqrt{2}\pi W (-2sF_2 - sF_3 - csF_4) \quad (23c)$$

$$L_4 = 4\sqrt{2}\pi W (2F_1 - 2cF_2 + s^2F_4), \quad (23d)$$

where the normalization factor  $4\sqrt{2}\pi W$  is important only for the total intensity and can be neglected as far as the polarizations are concerned.

Type	Observable	Definition	$M$ transform
Unpolarized	1	(000)	(122)
Single-pol.	$P$	(002)	(120)
"	$\Sigma$	(100)	(022)
"	$T$	(020)	(102)
Beam-target	$E$	(330)	(212)
"	$F$	(310)	-(232)
"	$G$	-(230)	(312)
"	$H$	-(210)	-(332)
Beam-recoil	$C_x$	(301)	(223)
"	$C_z$	(303)	-(221)
"	$O_x$	-(201)	(323)
"	$O_z$	-(203)	-(321)
Target-recoil	$T_x$	(011)	(133)
"	$T_z$	(013)	-(131)
"	$L_x$	(031)	-(113)
"	$L_z$	(033)	(111)

TABLE II: The definition of the 16 observables as the  $T_{lmn}$  correlations in Eq. 11. The defining  $T_{lmn}$  elements are listed as  $(lmn)$  in the third column and the corresponding  $M$  transformed elements are listed in the last column. Invariance under the  $M$  transform results in each observable occurring twice. The full intensity expansion is given in Eq. 24.

We emphasize again that our longitudinal amplitude formalism is essentially the same as the CGLN formalism. It may also be worth noting that the original CGLN work already pointed out that there are only four independent complex amplitudes. Aside from the extra factor of  $8\pi W$  in Eq. 20, our amplitudes match exactly with the CGLN matrix elements. The only difference between the  $L_i$ 's and the  $F_i$ 's is that the  $F_i$  amplitudes are computed in a particular reference frame, the c.m. frame, whereas the  $L_i$ 's are the invariant amplitudes, "as is". Therefore, the  $L_i$ 's can be computed in any reference frame.

## VII. THE POLARIZATION OBSERVABLES

We first define the sixteen observables as the various  $T_{lmn}$  elements (see Table II) noting that each observable occurs twice in the expansion given by Eq. 11. Our definitions for the observables follow those in FTS [3]. It is to be noted that there are minus signs in front of the defining  $T_{lmn}$  elements for the four double-polarization observables that use a linearly polarized beam ( $G$ ,  $H$ ,  $O_x$ , and  $O_z$ ). These extra sign flips are needed to preserve the definitions of these variables as *physical asymmetries*, as given in FTS [3]. The signs for  $G$ ,  $H$ ,  $O_x$ , and  $O_z$ , in terms of the *density matrix trace calculations*, as given in Appendix A in the FTS article will therefore acquire sign flips (see Sec. VII B and Sec. VII C for further details). We now write the full intensity profile in terms of the polarization observables as:

$$\begin{aligned}
\mathcal{I} = \mathcal{I}_0 \{ & (1 + P_x^S P_y^i P_y^b) + P(P_y^b + P_x^S P_y^i) + \Sigma(P_x^S + P_y^i P_y^b) + T(P_y^i + P_x^S P_y^b) + E(P_z^S P_z^i + P_y^S P_x^i P_z^b) \\
& + F(P_z^S P_x^i - P_y^S P_z^i P_y^b) + G(-P_y^S P_z^i + P_z^S P_x^i P_y^b) + H(-P_y^S P_x^i - P_z^S P_z^i P_y^b) + C_x(P_z^S P_x^b + P_y^S P_y^i P_z^b) \\
& + C_z(P_z^S P_z^b - P_y^S P_y^i P_x^b) + O_x(-P_y^S P_x^b + P_z^S P_y^i P_z^b) + O_z(-P_y^S P_z^b - P_z^S P_y^i P_x^b) + T_x(P_x^i P_x^b + P_x^S P_z^i P_z^b) \\
& + T_z(P_x^i P_z^b - P_x^S P_z^i P_x^b) + L_x(P_z^i P_x^b - P_x^S P_x^i P_z^b) + L_z(P_z^i P_z^b + P_x^S P_x^i P_x^b) \}. \quad (24)
\end{aligned}$$

We note that the three single polarizations ( $P$ ,  $\Sigma$  and  $T$ ) occur again as double correlations and the twelve double polarizations ( $E$ ,  $F$ ,  $G$ ,  $H$ ,  $C_x$ ,  $C_z$ ,  $O_x$ ,  $O_z$ ,  $T_x$ ,  $T_z$ ,  $L_x$  and  $L_z$ ) occur again as triple correlations.

### A. The 32 vanishing terms

The expansion in Eq. 11 has 64 terms, while Eq. 24 has only 32 terms. The rest of the 32 terms vanish under  $M$  invariance.  $T_{001}$  and  $T_{003}$  are examples of such terms (they do not occur in Table II). Physically, these two elements correspond to recoil polarizations (with unpolarized beam and target) along the  $\hat{x}$  and  $\hat{z}$  directions, which are required by  $M$  invariance to be zero. The general structure of these vanishing terms can be understood from the following example. From Eq. 14 for the photon, under a  $M$  transform,  $\sigma_1$  is connected to the identity matrix ( $\sigma_0$ ). Similarly, from Eqs. 14 and 16 for the baryons, it is  $\sigma_2$  that is connected to the identity matrix. We group  $\sigma_0$  and the Pauli matrix connected to  $\sigma_0$  by the  $M$  operator as “E” (type +1), and the rest ( $\sigma_2$  and  $\sigma_3$  for the photon, and  $\sigma_1$  and  $\sigma_3$  for the baryons) as of the “O” (type -1). A general correlation  $T_{lmn}$  vanishes if the product of the “types” of  $l$ ,  $m$ , and  $n$  is -1, since these are not invariant under the mirror symmetry transformation.

### B. Beam-target type experiments

We will show that our expressions for the intensity profiles as measured by the experimentalist conform to the definition of these observables as asymmetries. Following the notation set up in FTS [3] we will denote the cross-section for any configuration of the beam, target and recoil polarizations as  $\mathcal{I}^{(\gamma,i,b)}$ <sup>1</sup>. For beam-target type experiments,  $\vec{P}^b = \vec{0}$ , and Eq. 24 becomes

$$\begin{aligned}
\mathcal{I}^{(\gamma,i,0)} = \mathcal{I}_0 \{ & 1 + P_x^S \Sigma + P_x^i (-P_y^S H + P_z^S F) \\
& + P_y^i (T + P_x^S P) + P_z^i (-P_y^S G + P_z^S E) \} \quad (25)
\end{aligned}$$

The beam asymmetry is defined as

$$\Sigma = \frac{\mathcal{I}^{(\perp,0,0)} - \mathcal{I}^{(\parallel,0,0)}}{\mathcal{I}^{(\perp,0,0)} + \mathcal{I}^{(\parallel,0,0)}}, \quad (26)$$

where  $\parallel$  and  $\perp$  correspond to a beams with polarizations along the  $\hat{x}_{\text{evt}}$  ( $\phi = 0$ ) and  $\hat{y}_{\text{evt}}$  ( $\phi = \pi/2$ ) directions, respectively, and 0 denotes an unpolarized configuration. The target asymmetry is defined as

$$T = \frac{\mathcal{I}^{(0,+y,0)} - \mathcal{I}^{(0,-y,0)}}{\mathcal{I}^{(0,+y,0)} + \mathcal{I}^{(0,-y,0)}}, \quad (27)$$

and the four double polarizations are defined as

$$E = \frac{\mathcal{I}^{(r,+z,0)} - \mathcal{I}^{(r,-z,0)}}{\mathcal{I}^{(r,+z,0)} + \mathcal{I}^{(r,-z,0)}} \quad (28a)$$

$$F = \frac{\mathcal{I}^{(r,+x,0)} - \mathcal{I}^{(r,-x,0)}}{\mathcal{I}^{(r,+x,0)} + \mathcal{I}^{(r,-x,0)}} \quad (28b)$$

$$G = \frac{\mathcal{I}^{(+t,+z,0)} - \mathcal{I}^{(+t,-z,0)}}{\mathcal{I}^{(+t,+z,0)} + \mathcal{I}^{(+t,-z,0)}} \quad (28c)$$

$$H = \frac{\mathcal{I}^{(+t,+x,0)} - \mathcal{I}^{(+t,-x,0)}}{\mathcal{I}^{(+t,+x,0)} + \mathcal{I}^{(+t,-x,0)}}, \quad (28d)$$

where “ $r$ ” denotes a right-handed circularly polarized beam (all photons in the state  $|\epsilon_{\text{evt}}^+\rangle$ ), and “ $+t$ ” denotes a linearly polarized beam with  $\phi = +\pi/4$  with respect to  $\hat{x}_{\text{evt}}$ . The full expression for the cross-section in beam-target experiments reads

$$\begin{aligned}
\mathcal{I}_{\text{theory}}^{(\gamma,i,0)} = \mathcal{I}_0 \{ & 1 - P_L^\gamma \Sigma \cos(2\phi) + P_y^i (T - P_L^\gamma P \cos(2\phi)) \\
& + P_x^i (P_C^\gamma F + P_L^\gamma H \sin(2\phi)) \\
& + P_z^i (P_C^\gamma E + P_L^\gamma G \sin(2\phi)) \} \quad (29)
\end{aligned}$$

where we have added a subscript “theory” to remind the reader that this is for the theoretical formalism only. It can easily be checked that the definitions in Eqs. 26-28 are consistent with the intensity profile given by Eq. 29. Recall that  $\phi = +\pi/4$  corresponds to  $P_y^S = -1$  (see Table I), explaining the extra minus signs for  $G$  and  $H$  in the definitions of the corresponding  $T_{lmn}$  elements in Table II.

It is to be noted that one has access to an “extra” single-polarization observable, the recoil polarization  $P$ , even though the polarization of the recoiling baryon is not measured here. This is again due to the  $M$  transform relations. In fact, any double-polarization experiment has access to all the three single polarization observables. The definition of  $P$  as an asymmetry is given in the next sub-section.

<sup>1</sup> FTS defines the cross-section as  $\sigma^{(\gamma,i,b)}$ , whereas we define it as  $\mathcal{I}^{(\gamma,i,b)}$ , to avoid confusion with the Pauli  $\sigma$  matrices.

### C. Beam-recoil type experiments

For an experiment with beam and recoil baryon polarization information, we follow a similar logic. Here,  $\vec{P}^i = \vec{0}$ , and the beam-recoil expression is

$$\begin{aligned} \mathcal{I}_{\text{theory}}^{(\gamma,0,b)} = & \mathcal{I}_0 \{ 1 - P_L^\gamma \Sigma \cos(2\phi) + P_y^b (P - P_L^\gamma T \cos(2\phi)) \\ & + P_x^b (P_C^\gamma C_x + P_L^\gamma O_x \sin(2\phi)) \\ & + P_z^b (P_C^\gamma C_z + P_L^\gamma O_z \sin(2\phi)) \}, \end{aligned} \quad (30)$$

where the recoil polarization  $P$  is defined as

$$P = \frac{\mathcal{I}^{(0,0,+y)} - \mathcal{I}^{(0,0,-y)}}{\mathcal{I}^{(0,0,+y)} + \mathcal{I}^{(0,0,-y)}}. \quad (31)$$

The four beam-recoil double polarizations are

$$C_z = \frac{\mathcal{I}^{(r,0,+z)} - \mathcal{I}^{(r,0,-z)}}{\mathcal{I}^{(r,0,+z)} + \mathcal{I}^{(r,0,-z)}} \quad (32a)$$

$$C_x = \frac{\mathcal{I}^{(r,0,+x)} - \mathcal{I}^{(r,0,-x)}}{\mathcal{I}^{(r,0,+x)} + \mathcal{I}^{(r,0,-x)}} \quad (32b)$$

$$O_z = \frac{\mathcal{I}^{(+t,0,+z)} - \mathcal{I}^{(+t,0,-z)}}{\mathcal{I}^{(+t,0,+z)} + \mathcal{I}^{(+t,0,-z)}} \quad (32c)$$

$$O_x = \frac{\mathcal{I}^{(+t,0,+x)} - \mathcal{I}^{(+t,0,-x)}}{\mathcal{I}^{(+t,0,+x)} + \mathcal{I}^{(+t,0,-x)}}. \quad (32d)$$

The “extra” single polarization observable accessible here is the target asymmetry  $T$ , defined in Eq. 27.

As in the case of  $G$  and  $H$ , the definitions of  $O_x$  and  $O_z$  as asymmetries use  $\phi = +\pi/4$  that corresponds to  $P_y^S = -1$ . This explains the extra minus signs in the defining  $T_{lmn}$  elements in Table II for  $O_x$  and  $O_z$ .

### D. Target-recoil type experiments

The target-recoil expression is

$$\begin{aligned} \mathcal{I}^{(0,i,b)} = & \mathcal{I}^0 \{ 1 + P_y^i T + P_y^b (P + \Sigma P_y^i) \\ & + P_z^i (P_z^b L_z + P_x^b L_x) + P_x^i (P_x^b T_x + P_z^b T_z) \}, \end{aligned} \quad (33)$$

where the four target-recoil double polarizations are

$$T_z = \frac{\mathcal{I}^{(0,+x,+z)} - \mathcal{I}^{(0,+x,-z)}}{\mathcal{I}^{(0,+x,+z)} + \mathcal{I}^{(0,+x,-z)}} \quad (34a)$$

$$T_x = \frac{\mathcal{I}^{(0,+x,+x)} - \mathcal{I}^{(0,+x,-x)}}{\mathcal{I}^{(0,+x,+x)} + \mathcal{I}^{(0,+x,-x)}} \quad (34b)$$

$$L_z = \frac{\mathcal{I}^{(0,+z,+z)} - \mathcal{I}^{(0,+z,-z)}}{\mathcal{I}^{(0,+z,+z)} + \mathcal{I}^{(0,+z,-z)}} \quad (34c)$$

$$L_x = \frac{\mathcal{I}^{(0,+z,+x)} - \mathcal{I}^{(0,+z,-x)}}{\mathcal{I}^{(0,+z,+x)} + \mathcal{I}^{(0,+z,-x)}}. \quad (34d)$$

### VIII. CONNECTION WITH EXPERIMENTAL INTENSITY PROFILES

Until now, we have been careful to distinguish the “theoretical” intensity profiles from what experimentalists will actually measure. The only difference lies in the case of a linearly polarized beam where the laboratory analyzing direction set by the choice of the angle  $\theta$  (see Fig. 2) can vary. Eq. 33 remains the same between the theory and experimental formalisms, since it is independent of  $\theta$ . For Eqs. 29 and 30, however, we need to get back to the relation  $\phi = (\theta - \varphi)$  in Fig. 2. The easiest choice is to measure everything with respect to  $\hat{x}_{\text{lab}}$ , which usually represents the experimentalist’s choice of photon polarization axis. Therefore, we take  $\theta = 0$  (also called “para” setting), so that  $\phi = -\varphi$  and Eqs. 29 and 30 become

$$\begin{aligned} \mathcal{I}_{\text{para}}^{(\gamma,i,0)} = & \mathcal{I}_0 \{ 1 - P_L^\gamma \Sigma \cos(2\varphi) + P_y^i (T - P_L^\gamma P \cos(2\varphi)) \\ & + P_x^i (P_C^\gamma F - P_L^\gamma H \sin(2\varphi)) \\ & + P_z^i (P_C^\gamma E - P_L^\gamma G \sin(2\varphi)) \}, \end{aligned} \quad (35)$$

and

$$\begin{aligned} \mathcal{I}_{\text{para}}^{(\gamma,0,b)} = & \mathcal{I}_0 \{ 1 - P_L^\gamma \Sigma \cos(2\varphi) + P_y^b (P - P_L^\gamma T \cos(2\varphi)) \\ & + P_x^b (P_C^\gamma C_x - P_L^\gamma O_x \sin(2\varphi)) \\ & + P_z^b (P_C^\gamma C_z - P_L^\gamma O_z \sin(2\varphi)) \}, \end{aligned} \quad (36)$$

respectively. Similarly, for  $\theta = \pi/2$  (also called “perp” setting), we get

$$\begin{aligned} \mathcal{I}_{\text{perp}}^{(\gamma,i,0)} = & \mathcal{I}_0 \{ 1 + P_L^\gamma \Sigma \cos(2\varphi) + P_y^i (T + P_L^\gamma P \cos(2\varphi)) \\ & + P_x^i (P_C^\gamma F + P_L^\gamma H \sin(2\varphi)) \\ & + P_z^i (P_C^\gamma E + P_L^\gamma G \sin(2\varphi)) \}, \end{aligned} \quad (37)$$

and

$$\begin{aligned} \mathcal{I}_{\text{perp}}^{(\gamma,0,b)} = & \mathcal{I}_0 \{ 1 + P_L^\gamma \Sigma \cos(2\varphi) + P_y^b (P + P_L^\gamma T \cos(2\varphi)) \\ & + P_x^b (P_C^\gamma C_x + P_L^\gamma O_x \sin(2\varphi)) \\ & + P_z^b (P_C^\gamma C_z + P_L^\gamma O_z \sin(2\varphi)) \}. \end{aligned} \quad (38)$$

It is important to note that the sine and cosine terms in Eqs. 29 and 30 alter signs differently in going from the “theory” expressions to the “para” and “perp” settings, and this directly affects the signs of the extracted polarization observables. Therefore, care must be taken by the experimentalist to conform to a definition of the “para” and “perp” settings that matches with the theoretical definitions. Finally, we also note that it is beneficial to measure the intensity profiles for both the “para” and “perp” settings and extract the polarizations from the asymmetries between the two settings. This removes the overall normalization factor (the unpolarized cross-section), and therefore, any dependence on the detector acceptance (see Ref. [14] for details).



## IX. COMPUTATION OF POLARIZATION EXPRESSIONS IN THE LONGITUDINAL BASIS

### A. Some basic rules and caveats

We list some basic caveats that will be useful during the computations.

1. The matrix representation of an operator is  $\mathcal{O}_{nm} = \langle n|\mathcal{O}|m\rangle$  (note order of subscripts). For the Pauli matrices for example,  $(\sigma_y)_{+-} = -i$ ,  $(\sigma_z)_{--} = -1$ , etc.
2. FTS uses  $m_{s'}$  and  $m_s$  for outgoing baryon and incoming (target) spins. We adopt  $m_b$  and  $m_i$  as the final baryon and initial proton spins, respectively, and denote the photon spin by  $m_\gamma = \lambda$ . Any other index will be a dummy index for summation purposes. Also, unless otherwise mentioned, it is understood that repeated indices are to be summed over.
3. A useful relation is that for the conjugate operator  $J_\lambda^\dagger$ , the matrix elements are  $(J_\lambda^\dagger)_{m_i m_b} = (J_\lambda)_{m_b m_i}^* = \mathcal{A}_{\lambda m_b m_i}^*$ .
4. There are two types of traces in the FTS paper. “Tr” implies a trace over all spins, while “tr” implies a trace over the baryon spins, assuming that the photon spins have been traced over. To go from “Tr” to “tr”, that is, the procedure of doing the photon spin trace, is as follows. Let  $\Omega_b$  and  $\Omega_i$  be any operator in the final baryon and initial target proton spin space respectively. For the three Pauli matrices  $\sigma_x^\gamma$ ,  $\sigma_y^\gamma$  and  $\sigma_z^\gamma$ , the photon traces are computed as follows:

$$\begin{aligned} \text{Tr}[\Omega_b J \Omega_i \sigma_x^\gamma J^\dagger] &= \sum_{\lambda\lambda'} \text{tr}[\Omega_b J_\lambda \Omega_i (\sigma_x^\gamma)_{\lambda\lambda'} (J^\dagger)_{\lambda'\lambda}] \\ &= \text{tr}[\Omega_b J_+ \Omega_i (J^\dagger)_- + \Omega_b J_- \Omega_i (J^\dagger)_+] \end{aligned} \quad (39a)$$

$$\begin{aligned} \text{Tr}[\Omega_b J \Omega_i \sigma_y^\gamma J^\dagger] &= \sum_{\lambda\lambda'} \text{tr}[\Omega_b J_\lambda \Omega_i (\sigma_y^\gamma)_{\lambda\lambda'} (J^\dagger)_{\lambda'\lambda}] \\ &= -i \text{tr}[\Omega_b J_+ \Omega_i (J^\dagger)_- - \Omega_b J_- \Omega_i (J^\dagger)_+] \end{aligned} \quad (39b)$$

$$\begin{aligned} \text{Tr}[\Omega_b J \Omega_i \sigma_z^\gamma J^\dagger] &= \sum_{\lambda\lambda'} \text{tr}[\Omega_b J_\lambda \Omega_i (\sigma_z^\gamma)_{\lambda\lambda'} (J^\dagger)_{\lambda'\lambda}] \\ &= \text{tr}[\Omega_b J_+ \Omega_i (J^\dagger)_+ - \Omega_b J_- \Omega_i (J^\dagger)_-]. \end{aligned} \quad (39c)$$

Note that these expressions for the summations over the photon states are equivalent to those from the more conventional forms that can be found in Ref. [22], for example. The trace notation is simply a more compact way of expressing the spin sums.

5. Overall normalization factor. All 15 polarization observables will be normalized by the intensity factor  $\text{Tr}[JJ^\dagger]$ . This is given as

$$\text{Tr}[JJ^\dagger] = \sum_{\lambda m_i m_b} |\mathcal{A}_{\lambda m_i m_b}|^2. \quad (40)$$

This will not appear in our expressions below, but it is understood that this normalization always goes into the computations.

### B. The 15 polarization expressions

The detailed computation of the 15 polarizations are given below:

$$\begin{aligned} P &= \text{Tr}[\sigma_y^b J J^\dagger] \\ &= \langle m_b | \sigma_y | m'_b \rangle \langle m'_b | J_\lambda | m_i \rangle \langle m_i | J_\lambda^\dagger | m_b \rangle \\ &= \langle m_b | \sigma_y | m'_b \rangle \langle m'_b | J_\lambda | m_i \rangle (\langle m_b | J_\lambda | m_i \rangle)^* \\ &= -i \langle - | J_\lambda | m_i \rangle (\langle + | J_\lambda | m_i \rangle)^* + i \langle + | J_\lambda | m_i \rangle (\langle - | J_\lambda | m_i \rangle)^* \\ &= \sum_{\lambda m_i} -2 \text{Im} (\mathcal{A}_{\lambda m_i +} \mathcal{A}_{\lambda m_i -}^*) \end{aligned} \quad (41)$$

$$\begin{aligned} \Sigma &= \text{Tr}[J \sigma_x^\gamma J^\dagger] \\ &= \langle m_b | J_+ | m_i \rangle \langle m_i | J_-^\dagger | m_b \rangle + \langle m_b | J_- | m_i \rangle \langle m_i | J_+^\dagger | m_b \rangle \\ &= \langle m_b | J_+ | m_i \rangle (\langle m_b | J_- | m_i \rangle)^* + \langle m_b | J_- | m_i \rangle (\langle m_b | J_+ | m_i \rangle)^* \\ &= \sum_{m_i m_b} 2 \text{Re} (\mathcal{A}_{+m_i m_b} \mathcal{A}_{-m_i m_b}^*) \end{aligned} \quad (42)$$

$$\begin{aligned} T &= \text{Tr}[J \sigma_y^i J^\dagger] \\ &= -i \langle m_b | J_\lambda | + \rangle \langle - | J_\lambda^\dagger | m_b \rangle + i \langle m_b | J_\lambda | - \rangle \langle + | J_\lambda^\dagger | m_b \rangle \\ &= -i \langle m_b | J_\lambda | + \rangle (\langle m_b | J_\lambda | - \rangle)^* + i \langle m_b | J_\lambda | - \rangle (\langle m_b | J_\lambda | + \rangle)^* \\ &= \sum_{\lambda m_b} -2 \text{Im} (\mathcal{A}_{\lambda - m_b} \mathcal{A}_{\lambda + m_b}^*) \end{aligned} \quad (43)$$

$$\begin{aligned} E &= \text{Tr}[J \sigma_z^i \sigma_z^\gamma J^\dagger] \\ &= \langle m_b | J_+ | m'_b \rangle \langle m'_b | \sigma_z | m'_i \rangle \langle m'_i | J_+^\dagger | m_b \rangle \\ &\quad - \langle m_b | J_- | m'_b \rangle \langle m'_b | \sigma_z | m'_i \rangle \langle m'_i | J_-^\dagger | m_b \rangle \\ &= \langle m_b | J_+ | m'_b \rangle \langle m'_b | \sigma_z | m'_i \rangle (\langle m_b | J_+ | m'_i \rangle)^* \\ &\quad - \langle m_b | J_- | m'_b \rangle \langle m'_b | \sigma_z | m'_i \rangle (\langle m_b | J_- | m'_i \rangle)^* \\ &= \langle m_b | J_+ | + \rangle (\langle m_b | J_+ | + \rangle)^* - \langle m_b | J_+ | - \rangle (\langle m_b | J_+ | - \rangle)^* \\ &\quad - \langle m_b | J_- | + \rangle (\langle m_b | J_- | + \rangle)^* + \langle m_b | J_- | - \rangle (\langle m_b | J_- | - \rangle)^* \\ &= \sum_{m_b} (|\mathcal{A}_{++m_b}|^2 - |\mathcal{A}_{+-m_b}|^2 - |\mathcal{A}_{-+m_b}|^2 + |\mathcal{A}_{--m_b}|^2) \end{aligned} \quad (44)$$

$$\begin{aligned}
F &= \text{Tr}[J\sigma_x^i\sigma_z^\gamma J^\dagger] \\
&= \langle m_b|J_+|m'_b\rangle\langle m'_b|\sigma_x|m'_i\rangle\langle m'_i|J_+^\dagger|m_b\rangle \\
&\quad - \langle m_b|J_-|m'_b\rangle\langle m'_b|\sigma_x|m'_i\rangle\langle m'_i|J_-^\dagger|m_b\rangle \\
&= \langle m_b|J_+|m'_b\rangle\langle m'_b|\sigma_x|m'_i\rangle(\langle m_b|J_+|m'_i\rangle)^* \\
&\quad - \langle m_b|J_-|m'_b\rangle\langle m'_b|\sigma_x|m'_i\rangle(\langle m_b|J_-|m'_i\rangle)^* \\
&= \langle m_b|J_+|+\rangle(\langle m_b|J_+|-\rangle)^* + \langle m_b|J_+|-\rangle(\langle m_b|J_+|+\rangle)^* \\
&\quad - \langle m_b|J_-|+\rangle(\langle m_b|J_-|-\rangle)^* - \langle m_b|J_-|-\rangle(\langle m_b|J_-|+\rangle)^* \\
&= \sum_{m_b} 2\text{Re}(A_{++m_b}A_{+-m_b}^* - A_{-+m_b}A_{--m_b}^*) \quad (45)
\end{aligned}$$

$$\begin{aligned}
G &= -\text{Tr}[J\sigma_z^i\sigma_y^\gamma J^\dagger] \\
&= i\langle m_b|J_+|m'_b\rangle\langle m'_b|\sigma_z|m'_i\rangle\langle m'_i|J_-^\dagger|m_b\rangle \\
&\quad - i\langle m_b|J_-|m'_b\rangle\langle m'_b|\sigma_z|m'_i\rangle\langle m'_i|J_+^\dagger|m_b\rangle \\
&= i\langle m_b|J_+|m'_b\rangle\langle m'_b|\sigma_z|m'_i\rangle(\langle m_b|J_-|m'_i\rangle)^* \\
&\quad - i\langle m_b|J_-|m'_b\rangle\langle m'_b|\sigma_z|m'_i\rangle(\langle m_b|J_+|m'_i\rangle)^* \\
&= i\langle m_b|J_+|+\rangle(\langle m_b|J_-|+\rangle)^* - i\langle m_b|J_+|-\rangle(\langle m_b|J_-|-\rangle)^* \\
&\quad - i\langle m_b|J_-|+\rangle(\langle m_b|J_+|+\rangle)^* + i\langle m_b|J_-|-\rangle(\langle m_b|J_+|-\rangle)^* \\
&= \sum_{m_b} 2\text{Im}(A_{+-m_b}A_{--m_b}^* + A_{-+m_b}A_{++m_b}^*) \quad (46)
\end{aligned}$$

$$\begin{aligned}
H &= -\text{Tr}[J\sigma_x^i\sigma_y^\gamma J^\dagger] \\
&= i\langle m_b|J_+|m'_b\rangle\langle m'_b|\sigma_x|m'_i\rangle\langle m'_i|J_-^\dagger|m_b\rangle \\
&\quad - i\langle m_b|J_-|m'_b\rangle\langle m'_b|\sigma_x|m'_i\rangle\langle m'_i|J_+^\dagger|m_b\rangle \\
&= i\langle m_b|J_+|m'_b\rangle\langle m'_b|\sigma_x|m'_i\rangle(\langle m_b|J_-|m'_i\rangle)^* \\
&\quad - i\langle m_b|J_-|m'_b\rangle\langle m'_b|\sigma_x|m'_i\rangle(\langle m_b|J_+|m'_i\rangle)^* \\
&= i\langle m_b|J_+|+\rangle(\langle m_b|J_-|-\rangle)^* + i\langle m_b|J_+|-\rangle(\langle m_b|J_-|+\rangle)^* \\
&\quad - i\langle m_b|J_-|+\rangle(\langle m_b|J_+|-\rangle)^* - i\langle m_b|J_-|-\rangle(\langle m_b|J_+|+\rangle)^* \\
&= \sum_{m_b} 2\text{Im}(A_{--m_b}A_{++m_b}^* + A_{-+m_b}A_{+-m_b}^*) \quad (47)
\end{aligned}$$

$$\begin{aligned}
C_x &= \text{Tr}[\sigma_x^b J\sigma_z^\gamma J^\dagger] \\
&= \langle m_b|\sigma_x|m'_i\rangle\langle m'_i|J_+|m_i\rangle\langle m_i|J_+^\dagger|m_b\rangle \\
&\quad - \langle m_b|\sigma_x|m'_i\rangle\langle m'_i|J_-|m_i\rangle\langle m_i|J_-^\dagger|m_b\rangle \\
&= \langle m_b|\sigma_x|m'_i\rangle\langle m'_i|J_+|m_i\rangle(\langle m_b|J_+|m_i\rangle)^* \\
&\quad - \langle m_b|\sigma_x|m'_i\rangle\langle m'_i|J_-|m_i\rangle(\langle m_b|J_-|m_i\rangle)^* \\
&= \langle -|J_+|m_i\rangle(\langle +|J_+|m_i\rangle)^* - \langle -|J_-|m_i\rangle(\langle +|J_-|m_i\rangle)^* \\
&\quad + \langle +|J_+|m_i\rangle(\langle -|J_+|m_i\rangle)^* - \langle +|J_-|m_i\rangle(\langle -|J_-|m_i\rangle)^* \\
&= \sum_{m_i} 2\text{Re}(A_{+m_i}A_{+m_i}^* - A_{-m_i}A_{-m_i}^*) \quad (48)
\end{aligned}$$

$$\begin{aligned}
C_z &= \text{Tr}[\sigma_z^b J\sigma_z^\gamma J^\dagger] \\
&= \langle m_b|\sigma_z|m'_i\rangle\langle m'_i|J_+|m_i\rangle\langle m_i|J_+^\dagger|m_b\rangle \\
&\quad - \langle m_b|\sigma_z|m'_i\rangle\langle m'_i|J_-|m_i\rangle\langle m_i|J_-^\dagger|m_b\rangle \\
&= \langle m_b|\sigma_z|m'_i\rangle\langle m'_i|J_+|m_i\rangle(\langle m_b|J_+|m_i\rangle)^* \\
&\quad - \langle m_b|\sigma_z|m'_i\rangle\langle m'_i|J_-|m_i\rangle(\langle m_b|J_-|m_i\rangle)^* \\
&= \langle +|J_+|m_i\rangle(\langle +|J_+|m_i\rangle)^* - \langle +|J_-|m_i\rangle(\langle +|J_-|m_i\rangle)^* \\
&\quad - \langle -|J_+|m_i\rangle(\langle -|J_+|m_i\rangle)^* + \langle -|J_-|m_i\rangle(\langle -|J_-|m_i\rangle)^* \\
&= \sum_{m_i} (|A_{+m_i}|^2 - |A_{-m_i}|^2 - |A_{+m_i}|^2 + |A_{-m_i}|^2) \quad (49)
\end{aligned}$$

$$\begin{aligned}
O_x &= -\text{Tr}[\sigma_x^b J\sigma_y^\gamma J^\dagger] \\
&= i\langle m_b|\sigma_x|m'_i\rangle\langle m'_i|J_+|m_i\rangle\langle m_i|J_-^\dagger|m_b\rangle \\
&\quad - i\langle m_b|\sigma_x|m'_i\rangle\langle m'_i|J_-|m_i\rangle\langle m_i|J_+^\dagger|m_b\rangle \\
&= i\langle m_b|\sigma_x|m'_i\rangle\langle m'_i|J_+|m_i\rangle(\langle m_b|J_-|m_i\rangle)^* \\
&\quad - i\langle m_b|\sigma_x|m'_i\rangle\langle m'_i|J_-|m_i\rangle(\langle m_b|J_+|m_i\rangle)^* \\
&= i\langle -|J_+|m_i\rangle(\langle +|J_-|m_i\rangle)^* - i\langle -|J_-|m_i\rangle(\langle +|J_+|m_i\rangle)^* \\
&\quad + i\langle +|J_+|m_i\rangle(\langle -|J_-|m_i\rangle)^* - i\langle +|J_-|m_i\rangle(\langle -|J_+|m_i\rangle)^* \\
&= \sum_{m_i} 2\text{Im}(A_{-m_i}A_{+m_i}^* + A_{-m_i}A_{+m_i}^*) \quad (50)
\end{aligned}$$

$$\begin{aligned}
O_z &= -\text{Tr}[\sigma_z^b J\sigma_y^\gamma J^\dagger] \\
&= i\langle m_b|\sigma_z|m'_i\rangle\langle m'_i|J_+|m_i\rangle\langle m_i|J_-^\dagger|m_b\rangle \\
&\quad - i\langle m_b|\sigma_z|m'_i\rangle\langle m'_i|J_-|m_i\rangle\langle m_i|J_+^\dagger|m_b\rangle \\
&= i\langle m_b|\sigma_z|m'_i\rangle\langle m'_i|J_+|m_i\rangle(\langle m_b|J_-|m_i\rangle)^* \\
&\quad - i\langle m_b|\sigma_z|m'_i\rangle\langle m'_i|J_-|m_i\rangle(\langle m_b|J_+|m_i\rangle)^* \\
&= i\langle +|J_+|m_i\rangle(\langle +|J_-|m_i\rangle)^* - i\langle +|J_-|m_i\rangle(\langle +|J_+|m_i\rangle)^* \\
&\quad - i\langle -|J_+|m_i\rangle(\langle -|J_-|m_i\rangle)^* + i\langle -|J_-|m_i\rangle(\langle -|J_+|m_i\rangle)^* \\
&= \sum_{m_i} 2\text{Im}(A_{-m_i}A_{+m_i}^* + A_{+m_i}A_{-m_i}^*) \quad (51)
\end{aligned}$$

$$\begin{aligned}
T_x &= \text{Tr}[\sigma_x^b J\sigma_x^i J^\dagger] \\
&= \langle m_b|\sigma_x|m_i\rangle\langle m_i|J_\lambda|m'_i\rangle\langle m'_i|\sigma_x|m'_b\rangle\langle m'_b|J_\lambda^\dagger|m_b\rangle \\
&= \langle m_b|\sigma_x|m_i\rangle\langle m_i|J_\lambda|m'_i\rangle\langle m'_i|\sigma_x|m'_b\rangle(\langle m_b|J_\lambda|m'_b\rangle)^* \\
&= \langle -|J_\lambda|m'_i\rangle\langle m'_i|\sigma_x|m'_b\rangle(\langle +|J_\lambda|m'_b\rangle)^* \\
&\quad + \langle +|J_\lambda|m'_i\rangle\langle m'_i|\sigma_x|m'_b\rangle(\langle -|J_\lambda|m'_b\rangle)^* \\
&= \langle -|J_\lambda|+\rangle(\langle +|J_\lambda|-\rangle)^* + \langle +|J_\lambda|+\rangle(\langle -|J_\lambda|-\rangle)^* \\
&\quad + \langle -|J_\lambda|-\rangle(\langle +|J_\lambda|+\rangle)^* + \langle +|J_\lambda|-\rangle(\langle -|J_\lambda|+\rangle)^* \\
&= \sum_{\lambda} 2\text{Re}(A_{\lambda+}A_{\lambda-}^* + A_{\lambda+}A_{\lambda-}^*) \quad (52)
\end{aligned}$$

$$\begin{aligned}
T_z &= \text{Tr}[\sigma_z^b J \sigma_x^i J^\dagger] \\
&= \langle m_b | \sigma_z | m_i \rangle \langle m_i | J_\lambda | m'_i \rangle \langle m'_i | \sigma_x | m'_b \rangle \langle m'_b | J_\lambda^\dagger | m_b \rangle \\
&= \langle m_b | \sigma_z | m_i \rangle \langle m_i | J_\lambda | m'_i \rangle \langle m'_i | \sigma_x | m'_b \rangle (\langle m_b | J_\lambda | m'_b \rangle)^* \\
&= \langle + | J_\lambda | m'_i \rangle \langle m'_i | \sigma_x | m'_b \rangle (\langle + | J_\lambda | m'_b \rangle)^* \\
&\quad - \langle - | J_\lambda | m'_i \rangle \langle m'_i | \sigma_x | m'_b \rangle (\langle - | J_\lambda | m'_b \rangle)^* \\
&= \langle + | J_\lambda | + \rangle (\langle + | J_\lambda | - \rangle)^* - \langle - | J_\lambda | + \rangle (\langle - | J_\lambda | - \rangle)^* \\
&\quad + \langle + | J_\lambda | - \rangle (\langle + | J_\lambda | + \rangle)^* - \langle - | J_\lambda | - \rangle (\langle - | J_\lambda | + \rangle)^* \\
&= \sum_\lambda 2\text{Re}(\mathcal{A}_{\lambda++} \mathcal{A}_{\lambda-+}^* - \mathcal{A}_{\lambda+-} \mathcal{A}_{\lambda--}^*) \quad (53)
\end{aligned}$$

$$\begin{aligned}
L_x &= \text{Tr}[\sigma_x^b J \sigma_z^i J^\dagger] \\
&= \langle m_b | \sigma_x | m_i \rangle \langle m_i | J_\lambda | m'_i \rangle \langle m'_i | \sigma_z | m'_b \rangle \langle m'_b | J_\lambda^\dagger | m_b \rangle \\
&= \langle m_b | \sigma_x | m_i \rangle \langle m_i | J_\lambda | m'_i \rangle \langle m'_i | \sigma_z | m'_b \rangle (\langle m_b | J_\lambda | m'_b \rangle)^* \\
&= \langle - | J_\lambda | m'_i \rangle \langle m'_i | \sigma_z | m'_b \rangle (\langle + | J_\lambda | m'_b \rangle)^* + \\
&\quad \langle + | J_\lambda | m'_i \rangle \langle m'_i | \sigma_z | m'_b \rangle (\langle - | J_\lambda | m'_b \rangle)^* \\
&= \langle - | J_\lambda | + \rangle (\langle + | J_\lambda | + \rangle)^* + \langle + | J_\lambda | + \rangle (\langle - | J_\lambda | + \rangle)^* \\
&\quad - \langle - | J_\lambda | - \rangle (\langle + | J_\lambda | - \rangle)^* - \langle + | J_\lambda | - \rangle (\langle - | J_\lambda | - \rangle)^* \\
&= \sum_\lambda 2\text{Re}(\mathcal{A}_{\lambda+-} \mathcal{A}_{\lambda++}^* - \mathcal{A}_{\lambda--} \mathcal{A}_{\lambda-+}^*) \quad (54)
\end{aligned}$$

$$\begin{aligned}
L_z &= \text{Tr}[\sigma_z^b J \sigma_z^i J^\dagger] \\
&= \langle m_b | \sigma_z | m_i \rangle \langle m_i | J_\lambda | m'_i \rangle \langle m'_i | \sigma_z | m'_b \rangle \langle m'_b | J_\lambda^\dagger | m_b \rangle \\
&= \langle m_b | \sigma_z | m_i \rangle \langle m_i | J_\lambda | m'_i \rangle \langle m'_i | \sigma_z | m'_b \rangle (\langle m_b | J_\lambda | m'_b \rangle)^* \\
&= \langle + | J_\lambda | m'_i \rangle \langle m'_i | \sigma_z | m'_b \rangle (\langle + | J_\lambda | m'_b \rangle)^* \\
&\quad - \langle - | J_\lambda | m'_i \rangle \langle m'_i | \sigma_z | m'_b \rangle (\langle - | J_\lambda | m'_b \rangle)^* \\
&= \langle + | J_\lambda | + \rangle (\langle + | J_\lambda | + \rangle)^* - \langle - | J_\lambda | + \rangle (\langle - | J_\lambda | + \rangle)^* \\
&\quad - \langle + | J_\lambda | - \rangle (\langle + | J_\lambda | - \rangle)^* + \langle - | J_\lambda | - \rangle (\langle - | J_\lambda | - \rangle)^* \\
&= \sum_\lambda (|\mathcal{A}_{\lambda++}|^2 - |\mathcal{A}_{\lambda+-}|^2 - |\mathcal{A}_{\lambda-+}|^2 + |\mathcal{A}_{\lambda--}|^2) \quad (55)
\end{aligned}$$

### C. Expressions in terms of $L_i$ amplitudes

A summary of the expressions for the 16 observables in terms of the  $L_i$  amplitudes is given below:

$$\mathcal{N} = (|L_1|^2 + |L_2|^2 + |L_3|^2 + |L_4|^2) \quad (56a)$$

$$P = -2\text{Im}(L_1 L_2^* + L_4 L_3^*)/\mathcal{N} \quad (56b)$$

$$\Sigma = 2\text{Re}(L_1 L_3^* - L_4 L_2^*)/\mathcal{N} \quad (56c)$$

$$T = 2\text{Im}(L_1 L_4^* + L_2 L_3^*)/\mathcal{N} \quad (56d)$$

$$E = (|L_1|^2 + |L_2|^2 - |L_3|^2 - |L_4|^2)/\mathcal{N} \quad (56e)$$

$$F = 2\text{Re}(L_1 L_4^* + L_2 L_3^*)/\mathcal{N} \quad (56f)$$

$$G = -2\text{Im}(L_1 L_3^* - L_2 L_4^*)/\mathcal{N} \quad (56g)$$

$$H = 2\text{Im}(L_1 L_2^* + L_3 L_4^*)/\mathcal{N} \quad (56h)$$

$$C_x = 2\text{Re}(L_1 L_2^* + L_3 L_4^*)/\mathcal{N} \quad (56i)$$

$$C_z = (|L_1|^2 - |L_2|^2 - |L_3|^2 + |L_4|^2)/\mathcal{N} \quad (56j)$$

$$O_x = 2\text{Im}(L_1 L_4^* - L_2 L_3^*)/\mathcal{N} \quad (56k)$$

$$O_z = -2\text{Im}(L_1 L_3^* + L_2 L_4^*)/\mathcal{N} \quad (56l)$$

$$T_x = 2\text{Re}(L_1 L_3^* + L_2 L_4^*)/\mathcal{N} \quad (56m)$$

$$T_z = 2\text{Re}(L_1 L_4^* - L_2 L_3^*)/\mathcal{N} \quad (56n)$$

$$L_x = 2\text{Re}(L_1 L_2^* - L_3 L_4^*)/\mathcal{N} \quad (56o)$$

$$L_z = (|L_1|^2 - |L_2|^2 + |L_3|^2 - |L_4|^2)/\mathcal{N}, \quad (56p)$$

where  $\mathcal{N}$  is the normalization factor for the polarizations.

## X. THE CONSISTENCY RELATIONS

It is well known that the fifteen polarization observables occurring as bilinears in Eq. 56 can be connected by various identities. These are also called constraint equations, because they interconnect and place restrictions on the physical values these observables can take. Simply put, these equations are nothing but identities in the four independent amplitudes  $L_i$ . Chiang and Tabakin [4] have showed that these identities can be derived in a more sophisticated fashion by considering the complex space spanned by the four amplitudes. The observables can then be expanded in terms of the sixteen  $4 \times 4$  Dirac gamma matrix bilinears  $\{1, \gamma^\mu, \sigma^{\mu\nu}, \gamma^{\mu\nu\rho}, \gamma^{\mu\nu\rho\sigma}\}$  and the constraint relations emerge from the various Fierz identities connecting products of the Dirac bilinears. We list here the set of relations that we find to be valid while maintaining the equation-numbering as in Chiang-Tabakin [4]:

$$\begin{aligned}
1 &= \{\Sigma^2 + T^2 + P^2 + E^2 + G^2 + F^2 + H^2 \\
&\quad + O_x^2 + O_z^2 + C_x^2 + C_z^2 + L_x^2 + L_z^2 + T_x^2 + T_z^2\}/3 \quad (L.0)
\end{aligned}$$

$$\Sigma = TP + T_x L_z - T_z L_x \quad (L.\text{tr})$$

$$T = \Sigma P - (C_x O_z - C_z O_x) \quad (L.\text{br})$$

$$P = \Sigma T + GF - EH \quad (L.\text{bt})$$

$$G = PF + O_x L_x + O_z L_z \quad (L.1)$$

$$H = -PE + O_x T_x + O_z T_z \quad (L.2)$$

$$E = -PH + C_x L_x + C_z L_z \quad (L.3)$$

$$F = PG + C_x T_x + C_z T_z \quad (L.4)$$

$$O_x = TC_z + GL_x + HT_x \quad (L.5)$$

$$O_z = -TC_x + GL_z + HT_z \quad (L.6)$$

$$C_x = -TO_z + EL_x + FT_x \quad (L.7)$$

$$C_z = TO_x + EL_z + FT_z \quad (L.8)$$

$$T_x = \Sigma L_z + HO_x + FC_x \quad (L.9)$$

$$T_z = -\Sigma L_x + HO_z + FC_z \quad (L.10)$$

$$L_x = -\Sigma T_z + GO_x + EC_x \quad (L.11)$$

$$L_z = \Sigma T_x + GO_z + EC_z \quad (L.12)$$

$$0 = C_x O_x + C_z O_z - EG - FH \quad (Q.b)$$

$$0 = GH + EF - L_x T_x - L_z T_z \quad (Q.t)$$

$$0 = C_x C_z + O_x O_z - L_x L_z - T_x T_z \quad (Q.r)$$

$$0 = -\Sigma G + TF + O_z T_x - O_x T_z \quad (Q.\text{bt.1})$$

$$0 = -\Sigma H - TE - O_z L_x + O_x L_z \quad (\text{Q.bt.2})$$

$$0 = \Sigma E + TH - C_z T_x + C_x T_z \quad (\text{Q.bt.3})$$

$$0 = -\Sigma F + TG - C_z L_x + C_x L_z \quad (\text{Q.bt.4})$$

$$0 = -\Sigma O_x + PC_z - GT_z + HL_z \quad (\text{Q.br.1})$$

$$0 = -\Sigma O_z - PC_x + GT_x - HL_x \quad (\text{Q.br.2})$$

$$0 = -\Sigma C_x - PO_z - ET_z + FL_z \quad (\text{Q.br.3})$$

$$0 = -\Sigma C_z + PO_x + ET_x - FL_x \quad (\text{Q.br.4})$$

$$0 = TT_x - PL_z - HC_z + FO_z \quad (\text{Q.tr.1})$$

$$0 = TT_z + PL_x + HC_x - FO_x \quad (\text{Q.tr.2})$$

$$0 = TL_x + PT_z - GC_z + EO_z \quad (\text{Q.tr.3})$$

$$0 = TL_z - PT_x + GC_x - EO_x \quad (\text{Q.tr.4})$$

$$1 = G^2 + H^2 + E^2 + F^2 + \Sigma^2 + T^2 - P^2 \quad (\text{S.bt})$$

$$1 = O_x^2 + O_z^2 + C_x^2 + C_z^2 + \Sigma^2 - T^2 + P^2 \quad (\text{S.br})$$

$$1 = T_x^2 + T_z^2 + L_x^2 + L_z^2 - \Sigma^2 + T^2 + P^2 \quad (\text{S.tr})$$

$$0 = G^2 + H^2 - E^2 - F^2 - O_x^2 - O_z^2 + C_x^2 + C_z^2 \quad (\text{S.b})$$

$$0 = G^2 - H^2 + E^2 - F^2 + T_x^2 + T_z^2 - L_x^2 - L_z^2 \quad (\text{S.t})$$

$$0 = O_x^2 - O_z^2 + C_x^2 - C_z^2 - T_x^2 + T_z^2 - L_x^2 + L_z^2 \quad (\text{S.r})$$

These relations have been numerically verified by assigning random values to the four complex  $L_i$  amplitudes and calculating the polarizations employing Eqs. 56a-p. The relations consisting of only squares of the observables (Eqs. L.0 and S.bt-S.r) have no sign ambiguities. However, the signs in the remaining set of relations depend on the conventions adopted while defining the polarizations.

There appears to be some disagreement between different groups in the sign conventions for the polarizations, most likely arising from differences in the physics motivation. For example, in the CLAS  $C_x/C_z$  measurements for  $K^+\Lambda$  photoproduction [10], it was found that  $C_z \rightarrow +1$  at  $\vartheta_{\text{c.m.}}^{K^+} \rightarrow 0$  and  $C_z$  was seen as the spin-transfer from a right-handed circularly polarized photon to the recoiling baryon. Other groups [24] prefer to define  $C_z \rightarrow +1$  at  $\vartheta_{\text{c.m.}}^\Lambda \rightarrow 0$ , with the interpretation that  $C_z$  is the transfer of *helicity* from a right-handed circularly polarized photon to the  $\Lambda$ . Whatever be the choice of convention, the important issue is that the intensity profile the experimentalist uses must match with the asymmetry definitions that give the amplitude-level expressions. This point was detailed in Sec. VIII. We also note that except for a sign flip for the variable  $E$ , our consistency relations match those found by Sandorfi *et al.* in Ref. [6].

## XI. THE TRANSLATION “DICTIONARY”

In this work, we are following the FTS sign conventions as enlisted in Appendix A of the FTS paper [3]. It is important to note here that FTS first gives the definitions as *asymmetries*, with which we agree. Next, FTS

also gives their definitions in the density matrix language. As pointed out earlier in Secs. VIIB and VIIC, for the double-polarization observables with a linearly polarized beam, *viz.*,  $G$ ,  $H$ ,  $O_x$  and  $O_z$ , these FTS *density matrix expressions should have extra negative signs*. Therefore, except for these extra four sign flips, the conventions in this current work (CMU) agree with FTS.

To find how our signs relate to those from the work of other authors, the simplest way is to do a term-by-term check of what signs the different polarization observables carry in the full intensity expression. In our case, this is given by Eq. 24. Making comparisons with the corresponding expressions for SAID/MAID [24] and EBAC [6], we arrive at the following translation “dictionary” for the signs:

1. CMU/FTS  $\leftrightarrow$  SAID/MAID : flip signs of  $H$ ,  $E$ ,  $C_x$ ,  $C_z$ ,  $O_x$ ,  $O_z$  and  $L_x$ .
2. CMU/FTS  $\leftrightarrow$  EBAC : flip sign of  $E$ .

For the experimentalist, we urge that the particular sign convention chosen be clearly mentioned and care be taken that the “para” and “perp” definitions are correctly adhered to in going from  $\phi$  to  $\varphi$  (as defined in Fig. 2). Also, while showing the full intensity profile, it should be clearly mentioned which of the angles  $\phi$  and  $\varphi$  is being referred to.

## XII. SUMMARY AND OUTLOOK

We provide a detailed and self-contained description of the intensity profiles and amplitude-level expressions for the 15 polarization observables in pseudo-scalar meson photoproduction. Our calculations are based on the density-matrix approach of Fasano, Tabakin, and Saghai and our spin amplitudes have a universal spin-projection direction along the incident beam direction for all particles. We have also stressed the preservation of consistency between the sign-conventions of experiment and theoretical amplitude-level expressions. The current work is geared towards performing a mass-independent partial-wave analysis on the recently published CLAS data [9–12] and forthcoming results from JLab [14, 15].

## XIII. ACKNOWLEDGEMENTS

The authors thank Professor Reinhard Schumacher for his helpful comments during the preparation of this article. This work was supported in part by the US Department of Energy under Grant No. DE-FG02-87ER40315. D. Ireland also acknowledges the support of the United Kingdom’s Science and Technology Facilities Council.

- 
- [1] I. S. Barker, A. Donnachie and J. K. Storrow, Nucl. Phys. **B95**, 347 (1975).
  - [2] R. L. Walker, Phys. Rev. **182**, 1729 (1969).
  - [3] C. G. Fasano, F. Tabakin, and B. Saghai, Phys. Rev. C **46**, 2430 (1992).
  - [4] W.-T. Chiang and F. Tabakin, Phys. Rev. C **55**, 2054 (1997).
  - [5] D. Ireland, Phys. Rev. C **82**, 025204 (2010).
  - [6] A. M. Sandorfi, S. Hoblit, H. Kamano, T.-S. H. Lee, J. Phys. G: Nucl. Part. Phys. **38** 053001 (2011).
  - [7] G. F. Chew, M. L. Goldberger, F. E. Low and Y. Nambu, Phys. Rev. **106**, 1345 (1957).
  - [8] M. E. Peskin and D. V. Schroeder, *An Introduction to Quantum Field Theory*, Westview Press (1995).
  - [9] R. Bradford *et al.* (CLAS Collaboration), Phys. Rev. C **73**, 035202 (2006).
  - [10] R. Bradford *et al.* (CLAS Collaboration), Phys. Rev. C **75**, 035205 (2007).
  - [11] M. E. McCracken *et al.* (CLAS Collaboration), Phys. Rev. C **81**, 025201 (2010).
  - [12] B. Dey *et al.* (CLAS Collaboration), Phys. Rev. C **82**, 025202 (2010).
  - [13] M. Williams *et al.* (CLAS Collaboration), Phys. Rev. C **80**, 045213 (2009).
  - [14] Craig Paterson, *Polarization Observables in Strangeness Photoproduction with CLAS at Jefferson Lab*, Ph.D. Thesis, Glasgow University (2008).
  - [15] P. Eugenio *et al.* (CLAS Collaboration), *Search for Missing Nucleon Resonances in the Photoproduction of Hyperons Using A Polarized Photon Beam and A Polarized Target*, Jefferson Lab Experiment E02-112.
  - [16] A. Lleres *et al.*, Eur. Phys. J. A **31**, 79 (2007).
  - [17] A. Lleres *et al.*, Eur. Phys. J. A **39**, 149-161 (2009).
  - [18] K. Hicks *et al.*, Phys. Rev. C **76**, 042201 (2007).
  - [19] M. Sumihama *et al.*, Phys. Rev. C **73**, 035214 (2006).
  - [20] R. G. T. Zegers *et al.*, Phys. Rev. Lett. **91**, 092001 (2003).
  - [21] R. A. Adelseck and B. Saghai, Phys. Rev. C **42**, 108 (1990).
  - [22] G. R. Goldstein, J. F. Owens III, J. P. Rutherford, and M. J. Moravcsik, Nucl. Phys. **B80**, 164 (1974).
  - [23] X. Artru, M. Elchikh, J.-M. Richard, J. Soffer, and O. V. Teryaev, Phys. Rept., 470, 1 (2009).
  - [24] SAID database <http://gwdac.phys.gwu.edu/>; MAID database <http://wwwkph.kph.uni-mainz.de/MAID/>; for the SAID/MAID signs, we refer to Eqs. 13-15 in G. Knöchlein, D. Drechsel and L. Tiator, Z. Phys. A **352**, 327 (1995).